sciendo

Contemporary Agriculture, Vol. 73, No. 3-4 (2024): 157-164
DOI: https://doi.org/10.2478/contagri-2024-0019
UDC: 629.7.03

Original scientific paper

ISSN 2466-4774
https://www.contagri.info/

OPEN ACCESS

ASSESSING THE IMPACT OF UAV FLIGHT ALTITUDES ON THE ACCURACY OF MULTISPECTRAL INDICES

ZORAN STAMENKOVIĆ[1], *KRSTAN KEŠELJ*[1*], *MARKO KOSTIĆ*[1], *VLADIMIR AĆIN*[2], *DRAGANA TEKIĆ*[1], *MLADEN IVANIŠEVIĆ*[1], *TIHOMIR NOVAKOVIĆ*[1]

[1]Faculty of Agriculture, University of Novi Sad, Novi Sad, Serbia
[2]Institute of Field and Vegetable Crops, Novi Sad, Novi Sad, Serbia
**Corresponding author*: krstan.keselj@polj.uns.ac.rs

Submitted: 10.10.2023.
Reviewed: 20.08.2024.
Accepted: 06.09.2024.

SUMMARY

Precision agriculture has increasingly incorporated the use of Unmanned Aerial Vehicles (UAVs) equipped with multispectral cameras. This study examined the influence of different UAV flight altitudes on the Normalized Difference Vegetation Index (NDVI), Green Normalized Difference Vegetation Index (GNDVI), Normalized Difference Red Edge (NDRE), Optimized Soil-Adjusted Vegetation Index (OSAVI), and Leaf Chlorophyll Index (LCI), indices critical to crop monitoring and health assessment. The experiment was conducted on a 2-hectare winter wheat field at the Institute of Field and Vegetable Crops in Novi Sad, Serbia. The field was divided into 400 plots, each containing different wheat varieties subjected to twenty distinct combinations of artificial mineral fertilizer (NPK) treatments. A DJI P4 Multispectral drone was employed to capture images at altitudes of 30, 60, and 90 meters on three separate dates, corresponding to different plant growth stages: May 9, May 20, and June 6, 2022. All other operating parameters were held constant. The data were processed using the DJI Terra and Pix4D software to generate orthomosaic maps, which were subsequently analyzed using ArcGIS (v10.5, ESRI, Redlands, CA, USA) to calculate the multispectral index values for each plot. The results were statistically analyzed using the STATISTICA Tibco software. The analysis revealed significant differences in the index values based on the UAV flight altitude ($p < 0.05$). This research underscores the centrality of selecting the optimal UAV flight altitude to ensure the accuracy and reliability of data. While higher altitudes enable UAVs to cover larger areas in a single flight, factors such as image resolution, wind conditions, and the precision of crop health indicators must be considered. These findings offer valuable insights for agricultural professionals seeking to improve crop monitoring and ultimately enhance agricultural productivity through more effective UAV deployment.

Key words:
Unmanned Aerial Vehicles (UAVs), multispectral cameras, multispectral indices, UAVs flight altitude, crop monitoring, DJI P4 Multispectral

INTRODUCTION

The use of unmanned aerial vehicles (UAVs) for aerial photography has gained significant popularity, with recent technological advancements further increasing interest in their agricultural applications (Rasmussen et al., 2016; Otto et al., 2018). UAVs equipped with multispectral cameras have become especially valuable tools in precision agriculture (Primicerio et al., 2012; Rane & Choudhary, 2023).
Ivošević et al. (2023a, 2023b) conducted a comprehensive analysis of UAV applications in agriculture. Such UAVs can capture high-resolution images across multiple spectral bands, including the infrared range, enabling the detection of crop health, nutrient deficiencies, yield estimation, weather damage assessment, mapping, and pest

infestations monitoring and analysis (Jurado et al., 2020). Multispectral cameras, specialized for various applications, capture images that enable the calculation of several indices, with the most commonly used being the Normalized Difference Vegetation Index (NDVI), Normalized Difference Red Edge (NDRE), Green Normalized Difference Vegetation Index (GNDVI), Leaf Chlorophyll Index (LCI), and Optimized Soil-Adjusted Vegetation Index (OSAVI) (Jełowicki et. al., 2020; Liu, et. al., 2023; Szeląg et. al., 2023; Pipatsitee et. al., 2023).

To achieve optimal results, it is essential to determine the appropriate operating parameters, including flight height, image overlap, sensor calibration, and camera settings. Moreover, operational feasibility, such as battery consumption and flight time, must also be taken into account.

The selection of UAV flying altitude during image capture depends on the specific requirements of each application. When flying at higher altitudes, UAVs equipped with multispectral cameras experience a reduction in image resolution, as each pixel represents a larger ground area, leading to diminished detail and sharpness. Additionally, the overlap settings used for creating orthomosaic maps are closely linked to flight altitude. This issue was investigated by Mesas-Carrascosa et al. (2017), who examined the influence of UAV flight altitudes ranging from 30 to 90 meters above ground level, as well as different end-lap and side-lap settings (60-30% and 70-40%), on orthomosaic map accuracy. Their results indicated that the optimal spatial accuracy in bundle adjustment was achieved with a 70-40% overlap and flight altitudes between 60 and 90 meters.

Wind conditions also have a greater impact on the UAV flight stability when capturing images at higher altitudes. As the UAV ascends, it becomes more exposed to stronger and more unpredictable winds in the upper layers of the atmosphere, which can compromise flight stability and reduce image quality. However, flying at higher altitudes offers several advantages. The UAV can cover a larger surface area while maintaining the same battery consumption, thus saving time. Additionally, adjusting the UAV's speed can further optimize time efficiency, allowing for the capture of a wider area in a single flight. This is particularly beneficial for large-scale agricultural fields, forests, or other areas requiring extensive coverage (Njane et al., 2023).

Determining the optimal operating altitude for UAVs is critical to balancing factors such as image resolution, coverage area, and wind conditions, all of which are essential for achieving the desired results. Conducting tests and analyzing these trade-offs can help UAV operators identify the most suitable altitude for their specific applications, ensuring efficient and high-quality data acquisition. Similar issues were addressed by Mesas-Carrascosa et al. (2015), who described the technical specifications and configuration of a UAV for capturing remote images using a six-band multispectral sensor. Multiple flight missions were programmed at different altitudes (60, 80, and 100 m), with varying flight modes (stop and cruising), and ground control point (GCP) settings to analyze the impact of these parameters on the spatial resolution and spectral discrimination of multispectral orthomosaicked images processed using Pix4Dmapper. The study also emphasized the need to consider the coverage area and flight duration for each mission. The findings highlighted the importance of striking a balance between spatial resolution and spectral discrimination to optimize mission planning and image processing for achieving agronomic objectives. Specifically, spectral discrimination was evaluated for the detection of bare soil and vegetation (crops and weeds) to facilitate site-specific weed management during the growing season. The results demonstrated that users do not need to sacrifice coverage by flying at lower altitudes but can achieve an optimal balance between spatial resolution and spectral discrimination.

This study examined the influence of UAV flight altitude on the NDVI, GNDVI, NDRE, OSAVI and LCI values through statistical analysis, while maintaining all other operating parameters constant. The objective was to determine the most advantageous flight altitude for capturing imagery over wheat fields using the DJI P4 Multispectral UAV. In this context, the term "optimal" encapsulates various UAV metrics, including mission duration, energy efficiency in terms of battery consumption, spatial resolution of the acquired imagery, the extent of spatial coverage per flight, computational time required for data processing, resilience to meteorological variability, and geospatial accuracy.

MATERIAL AND METHODS

At the Institute of Field and Vegetable Crops in Novi Sad, on the Rimski Šančevi site (45°19'58.0"N 19°49'53.6"E), where the Department of Cereal Crops is located, a 2-hectare winter wheat experimental field was established. Photographic data from this field were collected on different dates and at distinct stages of plant growth: May 9, May 20, and June 6, 2022, using a DJI P4 Multispectral UAV equipped with a multispectral camera. The aerial surveys were conducted on sunny days between 12:00 and 13:00, which corresponds to solar noon. This time frame was selected to minimize potential errors caused by the spectral sensor's sensitivity to sunlight, as the sensor is mounted on top of the UAV. The data obtained from the surveys were processed using the DJI Terra and Pix4D software packages to generate an orthophoto map. The ArcGIS software package was then utilized to calculate the multispectral indices.

Experimental field

The 2-hectare field was divided into 400 small plots, each measuring 3 × 13.5 meters, as shown in Figure 1. A total of five wheat cultivars were sown: NS Igra, NS Rajna, NS Futura, NS Epoha, and NS Obala. The soil type at the site is Haplic Chernozem Aric (WRB, 2014), a highly fertile soil that dominates the Vojvodina region, accounting for approximately 43% of the total arable land (Jovanović et al., 2013). The study included five domestic high-yield winter wheat (*Triticum aestivum* L.) cultivars that are widely grown in Serbia: NS Igra, NS Rajna, NS Futura, NS Epoha, and NS Obala. These cultivars were selected for their high-yield potential and variation in plant height and grain quality traits. NS Igra is a new high-yield cultivar characterized by a lower habitus and good disease resistance. NS Obala and NS Rajna are awned cultivars known for their high yield stability. NS Futura is a taller cultivar, recognized for its premium grain quality, whereas NS Epoha is an awnless cultivar with stable yield and high grain quality. The experiment followed a split-plot design, with fertilizer treatments as the main factors and winter wheat cultivars as sub-factors. Each experimental plot was treated as an independent block (replicated three times), consisting of the five wheat cultivars arranged in a consistent order with randomized fertilizer treatments. Each cultivar received twenty different combinations of artificial mineral fertilizer (NPK), applied in four replicates. This experimental design effectively simulates diverse agricultural conditions, incorporating controlled variations in spectral channels to mirror natural fluctuations at a micro level. The field setup, with 400 plots representing the five wheat cultivars and twenty NPK treatment variations, allowed for the precise investigation of spectral responses under different conditions.

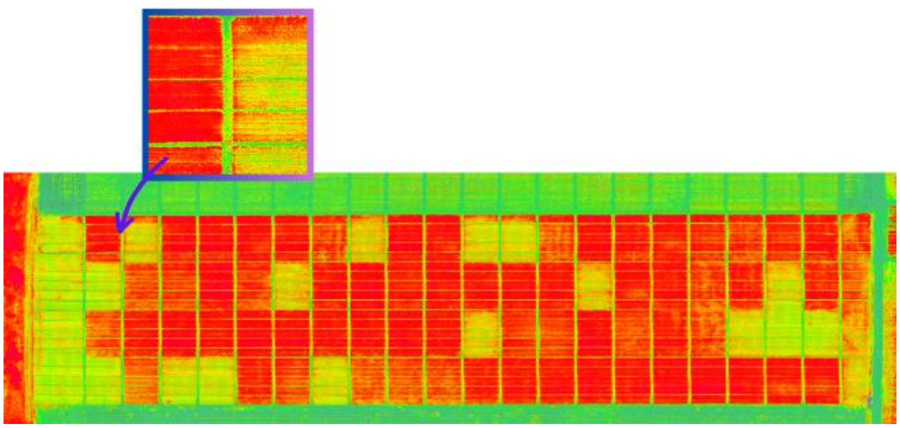

Figure 1. Orthophoto map of the experimental field captured using an RGB camera

This method enhances the accuracy of the experiment by enabling the artificial reproduction of naturally occurring phenomena. The variations in treatments involving the application of nitrogen (N), phosphorus (P), and potassium (K) fertilizers, as well as the combinations thereof, are presented in Table 1.

Table 1. Fertilizing treatments involving the application of N (nitrogen), P (phosphorus), and K (potassium)

Treatment	N (kg/ha)	P (kg/ha)	K (kg/ha)
1	0	0	0
2	100	0	0
3	0	100	0
4	0	0	100
5	100	100	0
6	100	0	100
7	0	100	100
8	50	50	50
9	50	100	50
10	50	100	100
11	100	50	50
12	100	100	50
13	100	100	100

14	100	150	50
15	100	150	150
16	150	50	50
17	150	100	50
18	150	100	100
19	150	150	100
20	150	150	150

Data acquisition using an unmanned aerial vehicle

The DJI P4 Multispectral unmanned aerial vehicle (UAV) is a quadcopter equipped with six 1/2.9" CMOS sensors: one RGB sensor and five monochromatic sensors, each with an effective resolution of 2.08 MP (2.12 MP in total). The camera is equipped with filters for Blue (B): 450 nm ± 16 nm, Green (G): 560 nm ± 16 nm, Red (R): 650 nm ± 16 nm, Red edge (RE): 730 nm ± 16 nm, and Near-infrared (NIR): 840 nm ± 26 nm.

Three imaging missions were conducted at altitudes of 30, 60, and 90 meters. The camera exposure was set to 2 seconds, with 5-meter margins, and a 75% frontal and 75% side overlap. Images were captured at equal time intervals, covering a total area of 27,800 square meters across all missions. The technical specifications of each mission are detailed in Table 2.

Table 2. Specifications of the executed missions

Altitude (m)	Mission Duration (s)	Resolution (cm/px)	Captured Area per Image (m²)	Number of Images per Channel	Total Number of Images per Mission	Flight Speed (m/s)	Distance Covered (m)	Avg. Wind Speed (m/s)
30	2,446	1.6	532.5	1,028	6,168	2.6	5,261	
60	665	3.2	2,130	280	1,680	5.2	2,864	1,2
90	320	4.8	4,792	134	804	7.7	2,068	

UAV multispectral data processing

For flight control, the UAV's spectral sensor of solar radiation was used to ensure an optimal flight path. The parameters such as ISO, white balance, and shutter speed were automatically adjusted based on the input from the solar radiation sensor, minimizing errors associated with manual adjustments. A single battery provides the UAV with a flight time of approximately 25–30 minutes during mission execution (Campi et al., 2019).

Following data acquisition with the DJI P4 Multispectral drone, the data was processed using both the DJI Terra (Su et al., 2021) and Pix4D (Olson et al., 2019) software packages. The implementation of both software tools allowed for the cross-verification of the results. The processing workflow included the generation of an orthomosaic map, which involves aligning and merging individual images to create a single, geometrically accurate representation of the experimental area. Georeferencing and photogrammetry techniques in DJI Terra and Pix4D ensured the precision and continuity of the imagery. Both software packages also applied algorithms for lens distortion correction, atmospheric correction, and color calibration, which improved image quality and provided accurate spectral values reflecting real-world field conditions.

After processing, the output consisted of a set of GeoTIFF files, i.e. georeferenced images containing metadata regarding the location and orientation of each pixel. These GeoTIFF files were subsequently imported into ArcGIS (Wilber et al., 2021) for further analysis. ArcGIS, an advanced Geographic Information System (GIS), facilitates detailed raster data analysis, including the calculation of multispectral indices for each parcel.

The equation used for calculating the multispectral indices is as follows (Herrmann et al., 2020; Qi et al., 2021; Lukas et al., 2022):

$$NDVI = \frac{NIR-R}{NIR+R} \quad (1)$$

$$GNDVI = \frac{NIR-G}{NIR+G} \quad (2)$$

$$NDRE = \frac{NIR-Red\ Edge}{NIR+Red\ Edge} \quad (3)$$

$$OSAVI = (1 + 0.16) \cdot \frac{(NIR - R)}{(NIR + R + 0.16)} \quad (4)$$

$$LCI = \frac{NIR - Red\ Edge}{NIR + R} \quad (5)$$

NIR refers to near-infrared, Red Edge represents near-red, whereas R and G correspond to the red and green segments of the spectrum.
The ArcGIS tools for raster data analysis were utilized to calculate the average multispectral indices values for each parcel (Fig. 2), allowing for quantitative comparisons of vegetation health between different treatments.

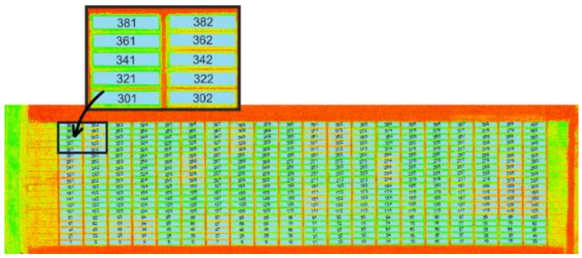

Figure 2. Extraction of NDVI values for 400 parcels using the ArcGIS software package

The visualization of multispectral indices values across the entire experimental field was accomplished using ArcGIS, which provided a visual representation of the vegetation health for each parcel. Throughout all the stages of this process, the preservation of data integrity was crucial to ensure that the analysis results accurately reflected real-world conditions in the field.

Statistical analysis
The STATISTICA software package, version 14.0.0.15 (Tibco Software Inc, Palo Alto, CA, USA, 2021), was used for statistical data processing. Initially, an F-test was applied to examine potential differences in the standard deviations of the observed indices across flight altitudes. This test was conducted to assess whether a statistically significant difference in the variability of multispectral indices existed at flight altitudes of 30 m, 60 m, and 90 m. The null hypothesis posits that the variances in multispectral indices across these altitudes are equivalent, indicating no significant differences. Conversely, the alternative hypothesis suggests distinct variances, implying notable differences in the precision of multispectral measurements at these specific altitudes. Following this, a one-way analysis of variance (ANOVA) was performed to determine whether statistically significant differences existed in the mean values of the observed indices across the flight altitudes. The fundamental premise underlying ANOVA is that no statistically significant divergence exists among the treatments applied in the study (Bewick et al., 2004). However, if the null hypothesis is rejected in favor of the alternative hypothesis, this would indicate statistically significant discrepancies between the treatments under investigation. To further identify the specific nature of these differences, a post-hoc analysis was conducted. The Tukey Honestly Significant Difference (HSD) test was selected for this post-hoc analysis, as it is a widely recognized method for all pairwise comparisons (Kim, 2015). All statistical tests were performed with a significance level of $\alpha = 0.05$.

RESULTS AND DISCUSSION

The F-test results for variance differences indicated statistically significant differences in the standard deviations across flight altitudes of 30, 60, and 90 m for all the indicators observed ($p < 0.05$).
After examining the differences in standard deviations, the differences in the arithmetic means of the various indices at flight altitudes of 30, 60, and 90 m were also assessed. The findings (p-values) are presented in Table 3, which summarizes the results from the analysis of variance (ANOVA). The table shows that the assumption of equality among treatments, specifically flight altitudes, can be statistically rejected for NDVI and OSAVI on the first measurement date and for NDVI on the third measurement date ($p < 0.05$). In all other cases, the initial hypothesis of equality of means across the observed treatments is accepted.

Table 3. ANOVA differences across flight altitudes of 30 m, 60 m, and 90 m for the specified measurement dates

MS Indices	**Measurement Dates**		
	09 May 2022	20 May 2022	06 June 2022

GNDVI	0.129	0.430	0.344
LCI	0.287	0.686	0.088
NDRE	0.497	0.516	0.453
NDVI	**0.044**	0.587	**0.003**
OSAVI	**0.019**	0.220	0.790

To test the significance of differences between pairs of treatments, the Tukey HSD test was applied (Tab. 4). This test was conducted only for indices where a statistically significant difference between pairs of treatments was observed, i.e. for NDVI and OSAVI.

Table 4. Tukey HSD test results

MS Indices	**Flight Height**	**Measurement Dates**								
		09 May 2022			20 May 2022			06 June 2022		
		30 m	60 m	90 m	30 m	60 m	90 m	30 m	60 m	90 m
NDVI	30 m	-	0.174	**0.042**	-	0.679	0.600	-	0.362	**0.002**
	60 m	0.174	-	0.808	0.679	-	0.991	0.362	-	0.096
	90 m	**0.042**	0.808	-	0.600	0.991	-	**0.002**	0.096	-
OSAVI	30 m	-	0.319	0.013	-	0.271	0.306	-	0.788	0.987
	60 m	0.319	-	0.351	0.271	-	0.997	0.788	-	0.871
	90 m	0.013	0.351	-	0.306	0.997	-	0.987	0.871	-

The results of the Tukey HSD test indicate that, during the first measurement date, a statistically significant difference in the NDVI values exists exclusively between the flight altitudes of 30 m and 90 m ($p < 0.05$). A similar conclusion applies to the third measurement date, where a statistically significant difference in the NDVI values was also found between these altitudes ($p < 0.05$). For OSAVI, statistically significant differences were observed only on the first measurement date between the flight altitudes of 30 m and 90 m ($p < 0.05$). These findings suggest that flight altitude can affect the NDVI and OSAVI values, underscoring the importance of carefully selecting altitude in studies utilizing these measurements.

Our findings are consistent with those of Stow et al. (2019), who reported that flight altitude significantly impacts reflectance, particularly in the near-infrared (NIR) band, with the NDVI values showing slight increases at higher altitudes. Their study noted that these effects were most pronounced within the first 25 meters above ground, stabilizing at higher altitudes. Similarly, our results demonstrated no significant differences in the NDVI and OSAVI values between 30 m and 60 m flights, suggesting that 50 m is an optimal flight height for reliable data acquisition without resorting to lower, more resource-intensive altitudes. Avtar et al. (2020) identified 60 m as the optimal altitude for accurately capturing biophysical parameters in oil palm plantations, balancing resolution and operational efficiency. Our study supports this finding, as we observed that 50 m provides comparable benefits, ensuring sufficient data accuracy while maximizing area coverage. Moreover, Jiang et al. (2020) emphasized that flight altitudes between 40 m and 100 m provide adequate resolution for vegetation indices in paddy rice fields, consistent with our finding that 50 m strikes a balance between image quality and operational efficiency.

CONCLUSION

This study examined the impact of varying flight altitudes of Unmanned Aerial Vehicles (UAVs) on the accuracy of multispectral indices critical for agricultural monitoring, with particular focus on the NDVI, GNDVI, NDRE, OSAVI, and LCI values.

Significant differences in the NDVI and OSAVI values were observed between flight altitudes of 30 m and 90 m. Statistical analysis, specifically the Tukey HSD test, revealed statistically significant differences in the NDVI values at these altitudes on the first and third measurement dates. For the other indices examined, including GNDVI, NDRE, and LCI, no significant statistical differences were found among flight altitudes, suggesting that altitude does not uniformly affect all multispectral indices.

While higher flight altitudes enable broader terrain coverage within a single flight, this study emphasizes the need to consider image resolution, UAV resilience to meteorological fluctuations, computational demands for data processing, and the accuracy of crop health indicators. Based on the findings, a flight altitude of 50 m is recommended as optimal, providing a balance between image quality and coverage efficiency without significantly impacting battery life or processing time.

These findings contribute valuable insights into the influence of UAV flight altitudes on the data quality within precision agriculture. The results obtained offer practical guidelines for farmers and specialists, enhancing UAV operation strategies for improved crop monitoring and analysis.

***Acknowledgements*:** This research was made possible through the invaluable support of Dron Agri D.O.O., Novi Sad, which generously provided the UAV and essential logistical assistance required for the successful execution of this study.

Authors' ORCID iDs:
Zoran Stamenković (https://orcid.org/0000-0003-2031-2688); Krstan Kešelj (https://orcid.org/0000-0002-4975-137X); Marko Kostić (https://orcid.org/0000-0001-9446-994X); Dragana Tekić (https://orcid.org/0000-0002-1924-6196); Mladen Ivanišević (https://orcid.org/0000-0003-4593-1485); Tihomir Novaković (https://orcid.org/0000-0002-8405-3403)

Conflict of interest: The authors declare that they have no conflict of interest.

REFERENCES

Avtar R., Suab S.A., Syukur M.S., Korom A., Umarhadi D.A., Yunus A.P. (2020): Assessing the influence of UAV altitude on extracted biophysical parameters of young oil palm. *Remote Sensing*, 12(18): 3030. https://doi.org/10.3390/rs12183030

Bewick V., Cheek L., Ball J. (2004): Statistics review 9: One-way analysis of variance. *Critical Care*, 8: 130. https://doi.org/10.1186/cc2836

Campi T., Cruciani S., Maradei F., Feliziani M. (2019): Innovative design of drone landing gear used as a receiving coil in wireless charging application. *Energies*, 12(18): 3483. https://doi.org/10.3390/en12183483

Herrmann I., Bdolach E., Montekyo Y., Rachmilevitch S., Townsend P.A., Karnieli A. (2020): Assessment of maize yield and phenology by drone-mounted superspectral camera. *Precision Agriculture*, 21: 51-76. https://doi.org/10.1007/s11119-019-09659-5

Ivošević B., Kostić M., Ljubičić N., Grbović Ž., Panić M. (2023a): Chapter 2 - A drone view for agriculture. In: Unmanned Aerial Systems in Agriculture. Bochtis D., Tagarakis A.C., Kateris D. (Eds.), Academic Press, pp. 25–47. https://doi.org/10.1016/B978-0-323-91940-1.00002-5

Ivošević B., Kostić M., Ljubičić N., Grbović Ž., Panić M. (2023b): Chapter 3 - Application of unmanned aerial systems to address real-world issues in precision agriculture. In: Unmanned Aerial Systems in Agriculture. Bochtis D., Tagarakis A.C., Kateris D. (Eds.), Academic Press, pp. 51-69. https://doi.org/10.1016/B978-0-323-91940-1.00003-7

Jełowicki L., Sosnowicz K., Ostrowski W., Osińska-Skotak K., Bakuła K. (2020): Evaluation of rapeseed winter crop damage using UAV-based multispectral imagery. *Remote Sensing*, 12(16): 2618. https://doi.org/10.3390/rs12162618

Jiang R., Wang P., Xu Y., Zhou Z., Luo X., Lan Y., Zhao G., Sanchez-Azofeifa A., Laakso K. (2020): Assessing the operation parameters of a low-altitude UAV for the collection of NDVI values over a paddy rice field. *Remote Sensing*, 12(11): 1850. https://doi.org/10.3390/rs12111850

Jovanović M., Pavić D., Mesaroš M., Stankov U., Pantelić M., Armenski T., Dolinaj D., Popov S., Ćosić Đ., Popović L., Frank A., Crnojević V. (2013): Water shortage and drought monitoring in Bačka region (Vojvodina, North Serbia) – setting-up measurement stations network. *Geographica Pannonica*, 17: 114-124.

Jurado J.M., Ortega L., Cubillas J.J., Feito F.R. (2020): Multispectral mapping on 3D models and multi-temporal monitoring for individual characterization of olive trees. *Remote Sensing*, 12(7): 1106. https://doi.org/10.3390/rs12071106

Kim H.-Y. (2015): Statistical notes for clinical researchers: *post-hoc* multiple comparisons. *Restorative Dentistry & Endodontics*, 40(2): 172. https://doi.org/10.5395/rde.2015.40.2.172

Liu S., Zhang B., Yang W., Chen T., Zhang H., Lin Y., Tan J., Li X., Gao Y., Yao S., Lan Y., Zhang L. (2023): Quantification of physiological parameters of rice varieties based on multi-spectral remote sensing and machine learning models. *Remote Sensing*, 15(2): 453. https://doi.org/10.3390/rs15020453

Lukas V., Huňady I., Kintl A., Mezera J., Hammerschmiedt T., Sobotková J., Brtnický M., Elbl J. (2022): Using UAV to identify the optimal vegetation index for yield prediction of oil seed rape (*Brassica napus* L.) at the flowering stage. *Remote Sensing*, 14: 4953. https://doi.org/10.3390/rs14194953

Mesas-Carrascosa F.J., Rumbao C.I., Torres-Sánchez J., García-Ferrer A., Peña J.M., López Granados F. (2017): Accurate ortho-mosaicked six-band multispectral UAV images as affected by mission planning for precision agriculture proposes. *International Journal of Remote Sensing*, 38(8-10): 2161-2176. http://doi.org/10.1080/01431161.2016.1249311

Mesas-Carrascosa F.-J., Torres-Sánchez J., Clavero-Rumbao I., García-Ferrer A., Peña J.-M., Borra-Serrano I., López-Granados F. (2015): Assessing optimal flight parameters for generating accurate multispectral orthomosaicks by uav to support site-specific crop management. *Remote Sensing*, 7: 12793-12814. https://doi.org/10.3390/rs71012793

Njane S.N., Tsuda S., van Marrewijk B.M., Polder G., Katayama K., Tsuji H. (2023): Effect of varying UAV height on the precise estimation of potato crop growth. *Frontiers in Plant Science*, 14: 1233349. https://doi.org/10.3389/fpls.2023.1233349

Olson D., Chatterjee A., Franzen D.W., Day S.S. (2019): Relationship of drone-based vegetation indices with corn and sugarbeet yields. *Agronomy Journal*, 111(5): 2545-2557. https://doi.org/10.2134/agronj2019.04.0260

Otto A., Agatz N., Campbell J., Golden B., Pesch E. (2018): Optimization approaches for civil applications of unmanned aerial vehicles (UAVs) or aerial drones: a survey. *Networks*, 72(4): 411-458. https://doi.org/10.1002/net.21818

Pipatsitee P., Tisarum R., Taota K. Samphumphuang A., Cha-um S. (2023): Effectiveness of vegetation indices and UAV-multispectral imageries in assessing the response of hybrid maize (*Zea mays* L.) to water deficit stress under field environment. *Environmental Monitoring and Assessment*, 195: 128. https://doi.org/10.1007/s10661-022-10766-6

Primicerio J., Di Gennaro S.F., Fiorillo E., Genesio L., Lugato E., Matese A., Vaccari F.P. (2012): A Flexible Unmanned Aerial Vehicle for Precision Agriculture. *Precision Agriculture*, 13(5): 517-523. https://doi.org/10.1007/s11119-012-9257-6

Qi H., Wu Z., Zhang L., Li J., Zhou J., Jun Z., Zhu B. (2021): Monitoring of peanut leaves chlorophyll content based on drone-based multispectral image feature extraction. *Computers and Electronics in Agriculture*, 187: 106292. https://doi.org/10.1016/j.compag.2021.106292

Rane N.L. & Choudhary S.P. (2023): Remote sensing (RS), UAV/drones, and machine learning (ML) as powerful techniques for precision agriculture: effective applications in agriculture. *International Research Journal of Modernization in Engineering Technology and Science*, 5(4): 4375-4392. https://www.doi.org/10.56726/IRJMETS36817

Rasmussen J., Ntakos G., Nielsen J., Svensgaard J., Poulsen R., Christensen S. (2016): Are vegetation indices derived from consumer-grade cameras mounted on UAVs sufficiently reliable for assessing experimental plots? *European Journal of Agronomy*, 74: 75-92. https://doi.org/10.1016/j.eja.2015.11.026

Stow D., Nichol C., Wade T., Jakob A., Gillian S., Helfter C. (2019): Illumination geometry and flying height influence surface reflectance and NDVI derived from multispectral UAS imagery. *Drones*, 3(3): 55. https://doi.org/10.3390/drones3030055

Su J., Yi D., Su B., Mi Z., Liu C., Hu X., Xu X., Guo L., Chen W.-H. (2020): Aerial visual perception in smart farming: field study of wheat yellow rust monitoring. *IEEE Transactions on Industrial Informatics,* 17(3): 2242-2249. 10.1109/TII.2020.2979237

Szeląg B., Sobura S., Stoińska R. (2023): Application of multispectral images from unmanned aerial vehicles to analyze operations of a wastewater treatment plant. *Energies*, 16(6): 2871. https://doi.org/10.3390/en16062871

Wilber A.L., Czarnecki J.M.P., McCurdy J.D. (2021): An ArcGIS Pro workflow to extract vegetation indices from aerial imagery of small-plot turfgrass research. *Crop Science*, 62: 503-511. https://doi.org/10.1002/csc2.20669

WRB (2014): World Reference Base for soil resources 2014: International soil classification system for naming soils and creating legends for soil maps. Food and Agriculture Organization of the United Nations, Rome. Available at: https://openknowledge.fao.org/server/api/core/bitstreams/bcdecec7-f45f-4dc5-beb1-97022d29fab4/content (Accessed: 1 September 2023).